CORROSION SCIENCE AND TECHNOLOGY, Vol.5, No.6(2006), pp.189~195

Effects of Tungsten on the Precipitation Kinetics of Secondary Phases and the Associated Susceptibility to Pitting Corrosion in Duplex Stainless Steels

†Chan-Jin Park[1] and Hyuk-Sang Kwon[2]

[1]School of Material Science and Engineering, Chonnam National University
300, Yongbong-dong, Buk-gu, Gwangju 500-757, Korea
[2]Department of Materials Science and Engineering,
Korea Advanced Institute of Science and Technology (KAIST)
373-1, Guseong-dong, Yuseong-gu, Daejeon 305-701, Korea

Effects of tungsten (W) on the precipitation kinetics of secondary phases and the associated resistance to pitting corrosion of 25 % Cr duplex stainless steels were investigated through microstructural and electrochemical noise analyses. With the partial substitution of W for Mo in duplex stainless steel, the potential and current noises of the alloy were significantly decreased in chloride solution due to retardation of the σ phase precipitation. The preferential precipitation of the χ phase in the W-containing alloy during the early period of aging contributed to retarding the precipitation of the σ phase by depleting W and Mo along grain boundaries. In addition, the retardation of the nucleation and growth of the σ phase in the W-containing alloy appears to be attributed to the inherently low diffusivity of W compared with that of Mo.

Keywords : duplex stainless steels; tungsten; secondary phase; electrochemical noise; pitting corrosion

1. Introduction

Austenitic-ferritic duplex stainless steel (DSS) is attractive as a structural material in the fields of energy/ environmental systems where both high mechanical strength and excellent resistance to localized and stress corrosion are required. Generally, these alloys have two to three times higher yield strength and exhibit greater resistance to localized and stress corrosion than type 300-series austenitic stainless steels at a comparable cost.[1)]

Commercial DSS usually contain 22-25 % Cr, 5-7 % Ni, 3-4 % Mo and 0.15-0.35 % N, and recent trends for newly developed DSS are towards increasing the Cr and Mo contents of the alloys to improve the resistance to localized and stress corrosion. However, the increase in Cr and Mo contents in DSS promotes the precipitation of secondary phases such as sigma (σ), chi (χ), chromium nitrides, and alpha prime (α′) phases when exposed to temperatures of 300 ~ 900 ℃[1)-3)]. Above all, the σ phase, a body-centered, tetragonal intermetallic compound that is rich in Cr and Mo with a larger volume fraction than any other phases is considered as the most detrimental secondary phase in DSS.

It is well known that the mechanical properties of DSS can be seriously deteriorated by the formation of small amount of σ phase.[3),6)] Thus, the production of thick pipes or bars with large diameters is limited because of the precipitation of the σ phase in the interior of products where cooling rate is relatively slow after solution annealing treatment. The precipitation of σ phase also depletes surrounding phases of Cr and Mo, leading to a reduction in corrosion resistance of DSS.[6)-9)]

Kim et al. previously reported that the resistance to pitting and stress corrosion of 25 % Cr DSS was significantly degraded with aging at 850 ℃.[10)] They suggested that the deterioration in resistance to localized corrosion of the alloy is due to the precipitation of σ phase at austenite (γ)/ferrite (α) or ferrite (α)/ferrite (α) boundaries, and additionally the precipitation kinetics of such a phase can be delayed by partial substitution of tungsten (W) for molybdenum (Mo) in DSS. In spite of a large body of previous studies on the effects of secondary on the corrosion resistance of DSS, few attempts have been systematically made to study how tungsten affects the precipitation of secondary phases and the associated initiation and propagation of pitting corrosion. In addition, to gain infor-

†Corresponding author: parkcj@chonnam.ac.kr

mation on the initial stage of pitting, especially on metastable pitting, near the secondary phase is very important to understand the effect of such phase on the localized or stress corrosion of DSS.

Recently, electrochemical noise measurement (ENM) technique has been widely used in studies on the pit stability of conventional austenitic stainless steels.[11)-14)] In particular, the potential or current transients in the time domain are closely associated with the initiation and following repassivation of metastable pits. However, thus far, research on pitting in DSS using electrochemical noise measurements (ENM) has rarely been conducted.

The aim of the present study is to investigate the effects of precipitation kinetics of secondary phases and the associated susceptibility to pitting corrosion through microstructural and electrochemical noise analyses.

2. Experimental

The alloys used in this work were melted in a vacuum induction furnace, and cast in 25 kg ingot. The chemical compositions of the alloys are presented in Table 1. The alloys were designed to have chemical compositions of Fe-25Cr-7Ni-3Mo-0.25 N and Fe-25Cr-7Ni-3W-1.5Mo-0.25N respectively, with same PREN (42=%Cr+3.3 (%Mo+0.5%W)+30%N) value. Each alloy was named 3Mo and 3W-1.5Mo according to its Mo and/or W compositions. The alloys were prepared in the form of a hot-rolled sheet 4 mm thick after homogenization heat treatment for 2 h at 1250 ℃. Then, the alloys were solution annealed for 2 h at 1050 ℃, and finally aged respectively for 10 min, 20 min, 1 h, and 10 h at 850 ℃. The specimens were ground with silicon carbide paper up to 2000 mesh finish before electrochemical tests. Some specimens were polished to 1 μm finish before testing for metallographic observations.

Electrochemical potential and current noises of the alloys were measured in 10% $FeCl_3 \cdot 6H_2O$ solution at 60 ℃ with a sampling time of 1 s for data acquisition, and then quantitatively analyzed by the maximum entropy method (MEM).[15)] To measure the critical pitting temperature (CPT) and electrochemical noise, a zero resistance ammetry (ZRA) was used, as reported in reference.[16),17)] The working electrode with an exposure area of 0.5 cm^2 was coupled with a thin platinum (Pt) wire with a tip diameter of about 100 μm, and both electrodes were connected via a ZRA. Thin Pt wire was used as a cathode to reduce the contaminating noise from the cathode and to minimize the shift of corrosion potential of the working electrode affected by the inert noble electrode.[17)] Electrochemical cell was enclosed in a shielding box composed of inner layer of styrofoam insulator and outer layer of copper shield to maintain the solution temperature and to protect the system from external noises. During the CPT measurements solution temperature was increased at a rate of 0.8 ℃ · min^{-1}.

Microstructure and phase composition of the alloy were examined by scanning electron microscope (SEM) with back-scattering detector and by an attached electron-dispersive X-ray spectroscope (EDS).

Table 1. Chemical compositions (wt. %) of the duplex stainless steels.

	Cr	Ni	Mo	W	N	Fe
3Mo	24.60	6.60	3.12	-	0.25	bal.
3W-1.5Mo	24.82	6.79	1.60	3.25	0.25	bal.

3. Results and discussion

3. 1 Influence of tungsten (W) on the precipitation kinetics of secondary phases

Fig. 1 shows the back-scattered electron (BSE) images of 3Mo (Fe-25Cr-7Ni-3Mo-0.25N) and 3W-1.5Mo (Fe-25Cr-7Ni-3W-1.5Mo-0.25N) alloys aged at 800 ℃. In addition, the volume fractions of secondary phases in the alloys are represented in Fig. 2. Compared with 3Mo alloy, Mo was partially substituted by W in 3W-1.5Mo alloy. With aging for 20 min, fine χ phase precipitated continuously along grain boundaries in 3W-1.5Mo alloy, while relatively larger σ phase appeared mainly at grain boundary triple points in 3Mo alloy. χ phase can be easily distinguished from σ phase, since it is brighter than σ phase in BSE image due to its higher Mo and/or W contents than σ phase. In addition, the volume fraction of χ phase in 3W-1.5Mo alloy and that of σ phase in 3Mo alloy increased with increasing aging time to 20 min. In the 3W-1.5Mo alloy aged for 1 h, σ. phase was also visible around χ phase in company with an increase in volume fraction of χ phase. There was also an increase in volume fraction of σ phase for 3Mo alloy. However, the volume fraction of χ phase in 3W-1.5Mo alloy decreased with an aging for longer than 1 h. Instead, the volume fraction of σ phase increased significantly. With an aging for 10 h, the volume fraction of σ phase in 3W-1.5Mo alloy exceeded that in 3Mo alloy, while the χ phase in 3W-1.5Mo alloy almost disappeared. The 3W-1.5Mo alloy was free from the precipitation of σ phase until aged for 20 min, and the volume fraction of σ phase of 3W-1.5Mo alloy was much smaller than that of 3Mo alloy even with an aging for 1h. Instead, χ phase was mainly found in 3W-1.5Mo alloy in an early stage of aging, while such

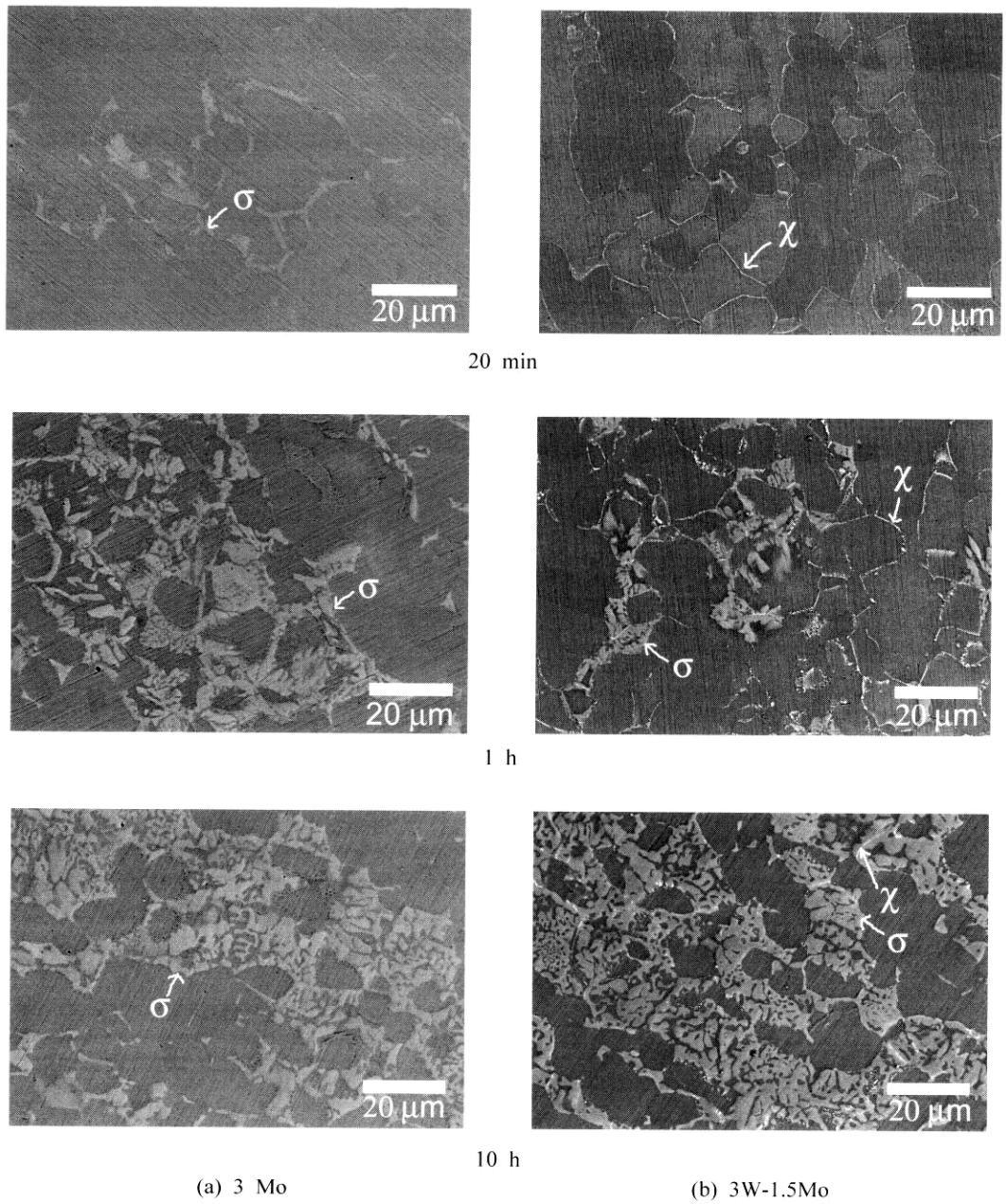

Fig. 1. Back-scattered electron images of (a) 3Mo and (b) 3W-1.5Mo alloys aged respectively for 20 min, 1h, and 10 h at 800 ℃.

phase was not visible in the 3Mo alloy. The precipitation of χ phase appears to be closely associated with the retardation of the precipitation σ phase.

Table 2 shows the chemical compositions of σ and χ phases in the 3Mo and 3W-1.5Mo alloys aged for 20 min at 800 ℃. The σ phases of each alloy were richer in Cr, Mo and/or W than matrix. For the χ phase observed only in 3W-1.5Mo alloy, the Cr contents were lower, but Mo and W contents were higher than the σ phase instead. In particular, the χ phase exhibited much higher W contents, 8.09 % compared to that, 3.47 % in the σ phase, while the difference in Mo contents between σ and χ phase was relatively small. Accordingly, during aging, W appears to preferentially segregate in χ phase rather than in σ. In other words, W should be a strong stabilizer for χ phase.

Two possible mechanisms were suggested in the previous study to explain the reason why the precipitation of σ phase is delayed for the W-containing alloys in early stage of aging.[1),10)] Since the formation of σ phase in the 3W-1.5Mo alloy requires high concentrations of Mo and/or

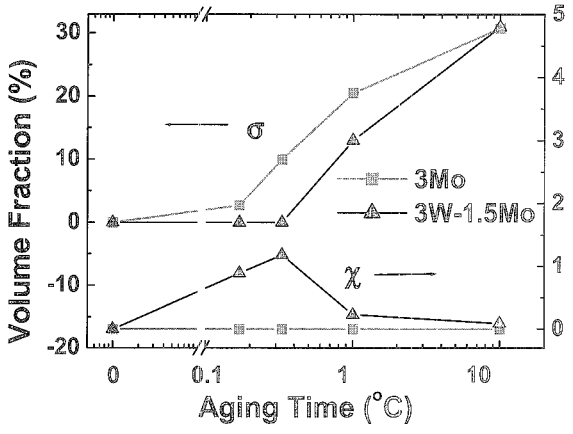

Fig. 2. Effect of aging at 800 ℃ on the volume fractions of σ and χ phases of 3W-1.5Mo and 3Mo alloys.

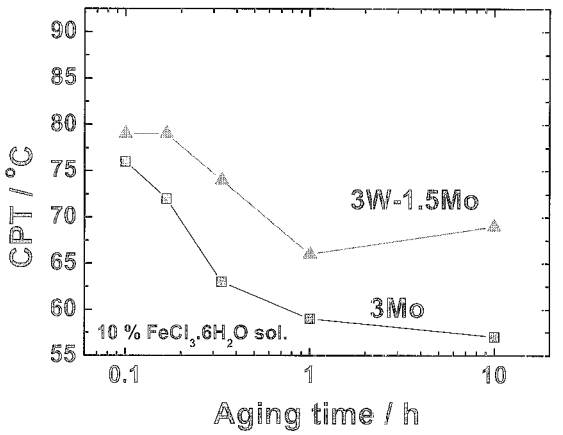

Fig. 3. Effect of aging at 800 ℃ on the CPT of 3Mo and 3W-1.5Mo alloys in 10 % $FeCl_3 \cdot 6H_2O$ solution.

Table 2. Chemical compositions of secondary phases in 3Mo and 3W-1.5Mo alloy aged for 20 min at 800 ℃.

Alloy	3Mo		3W-1.5Mo		
Phase	Overall	σ	Overall	σ	χ
Cr	24.6	30.34	24.82	30.92	25.75
Mo	3.12	8.12	1.6	5.22	6.71
W	-	-	3.25	3.7	8.09
Ni	6.6	4.1	6.79	3.29	5.08
Fe	bal.	bal.	bal.	bal.	bal.

W, the preferential precipitation of χ phase in the alloy during the initial period of aging can inhibit the nucleation and growth of σ phase by depleting W and Mo adjacent to the χ precipitates. In addition, the retardation of the nucleation and growth of the σ phase in 3W-1.5Mo alloy may be attributed to the inherent difference in diffusion rate between W and Mo. It was previously reported that the diffusion rate of W at 800 ℃ was 10 to 100 times slower than that of Mo in iron and ferrous alloys.[18)-20)]

3.2 Influence of tungsten (W) on critical pitting temperature

Fig. 3 shows the effect of aging on the critical pitting temperature (CPT) of 3Mo and 3W-1.5Mo alloys. On the whole, the CPTs of 3Mo and 3W-1.5Mo alloys were found to decrease with increasing aging time. The 3Mo alloy exhibited poorer resistance to pitting corrosion and severer degradation in CPT with aging than the 3W-1.5Mo alloy did. It is noticeable that the aging time when the first decrease in CPT was observed corresponds to when the σ phase appeared first. This suggests that the degradation in CPT is mainly due to the precipitation of σ phase in the alloys. Fig. 3 also shows the slight recovery of CPT after aging for 1h, especially for 3W-1.5Mo alloy, though the volume fraction of σ phase increased as shown in Fig. 2. This appears to be the replenishment of Cr and Mo from the surrounding matrix by over-aging.

3.3 Influence of tungsten (W) on electrochemical noise

Fig. 4 shows the effect of aging on the potential and current noises for solution annealed and the aged alloys. The corresponding PSD plots were also shown in Fig. 5. For the solution annealed condition, the potential of 3W-1.5Mo alloy was stable overall near at 630 mV while the potential of 3Mo alloy fluctuated between more active 490 and 520 mV. Furthermore, the mean current of 3Mo alloy was measured to be higher than that of 3W-1.5Mo alloy. The PSD in low frequency also confirmed that the electrochemical noises resulting from film reakdown process were reduced by the partial substitution of W (3W-1.5Mo) for Mo (3Mo alloy) in DSS. With increasing aging time to 20 min, the potential and current of both alloys fluctuated more severely than those of the solution annealed alloys. With aging for longer than 1h, both 3Mo and 3W-1.5Mo alloy exhibited stable pitting corrosion behavior. Potential belonged to active region and current exceeded the value of 100 μA. The PSD of 3Mo alloy was higher than that of 3W-1.5Mo alloy in most aged condition except the highly aged for 10 h. The higher PSD indicates the higher severity of localized corrosion, and the localized corrosion is closely associated with the precipitation of secondary phase, especially σ phase. The precipitation of σ phase was delayed by the partial substitution of W for Mo. This was also confirmed in electrochemical noises by the reduction in electrochemical noises and associated PSD by the partial substitution of W for Mo.

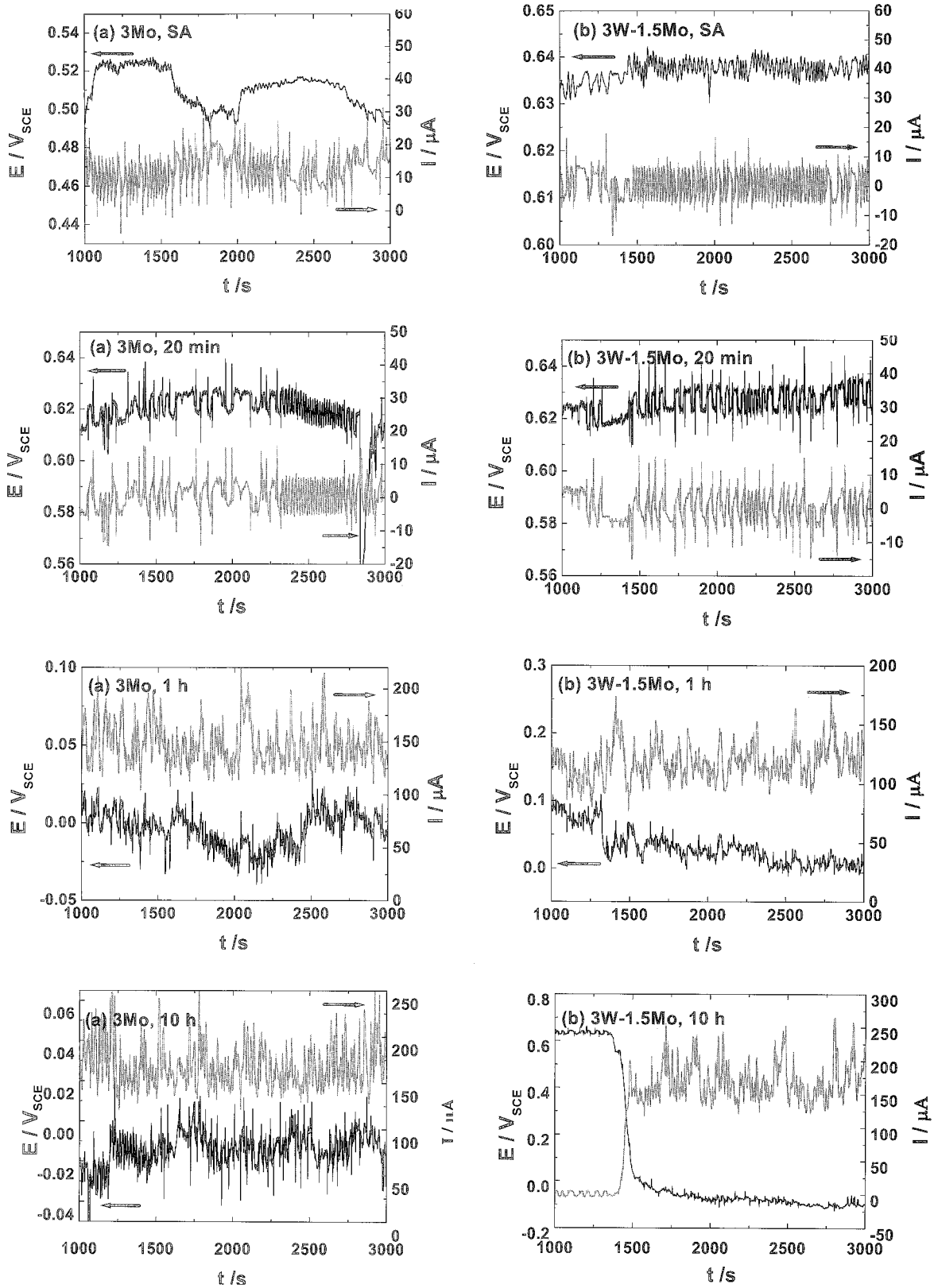

Fig. 4. Potential and current noises of 3Mo and 3W-1.5Mo alloys which were solution annealed and aged for 20 min, 1 h and 10 h, respectively, in 10 % $FeCl_3 \cdot 6H_2O$ solution at 60 ℃.

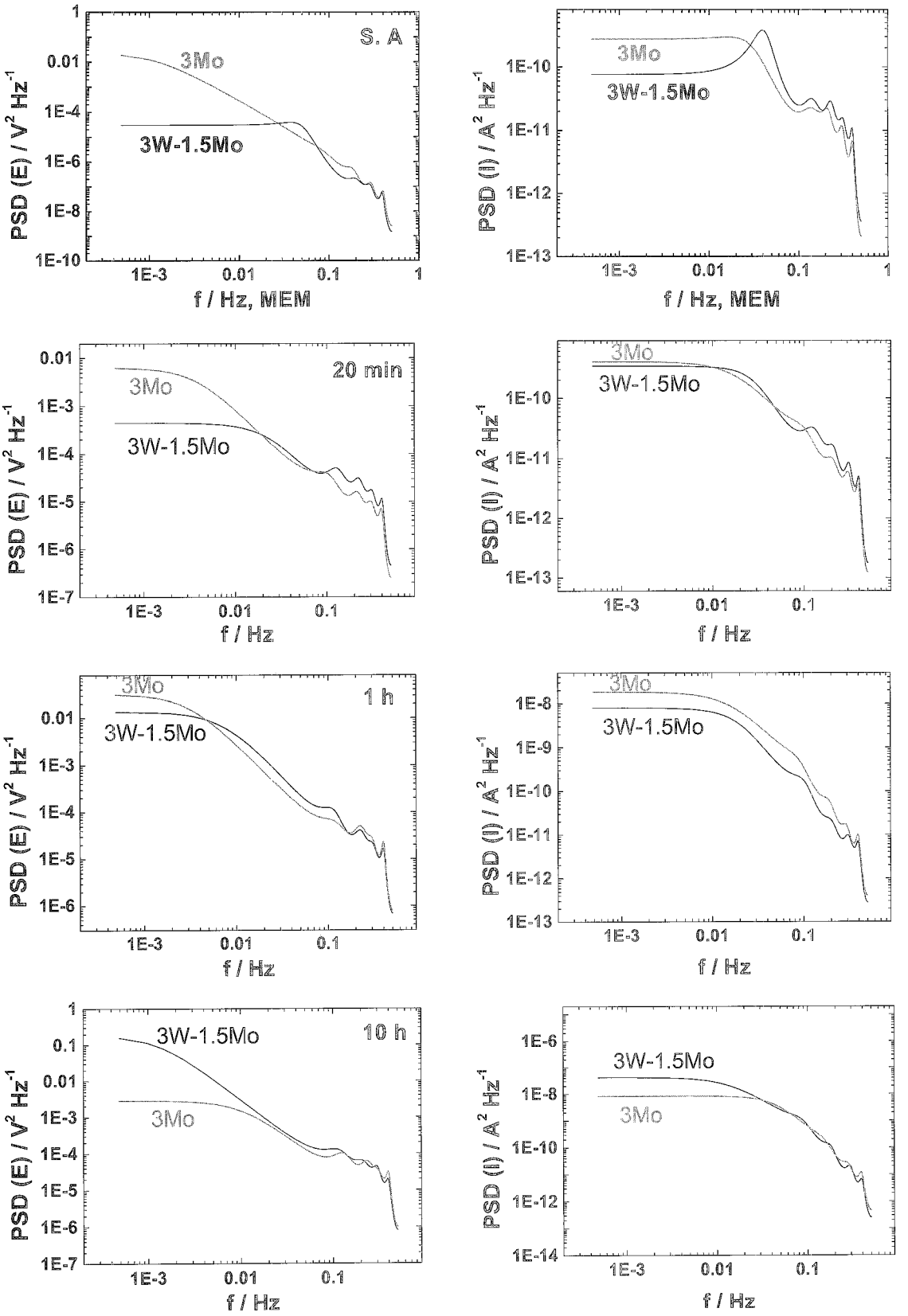

Fig. 5. Potential and current PSD corresponding to the potential and current noises of 3Mo and 3W-1.5Mo alloys which were solution annealed and aged for 10 min, 20 min, 1 h and 10 h.

4. Conclusions

1. W in DSS appears to be a strong stabilizer for χ phase with high contents of Mo and W. The preferential precipitation of the χ phase in the W-containing alloy during the early stage of aging contributed to retarding the precipitation of the σ phase by depleting W and Mo along grain boundaries. In addition, since the σ phase in the 3W-1.5Mo alloy contained relatively high content of W, the nucleation and growth of the σ phase may be delayed due to the inherently low diffusivity of W compared with that of Mo.

2. CPTs of the 3Mo and 3W-1.5Mo alloys decreased with aging due mainly to the precipitation of σ phase. However, the degradation of CPT was retarded for the 3W-1.5Mo alloy compared with that for 3Mo alloy, resulting from the delay in the precipitation of the σ phase by the partial substitution of Mo for W in the alloy.

3. The potential and current noises, which were associated with the initiation and the following repassivation of metastable pitting, and the corresponding PSD of 3Mo and 3W-1.5Mo alloys increased with aging due to the precipitation of σ phase. However, 3W-1.5Mo alloy showed better resistance to the initiation of pitting corrosion than 3Mo alloy in an early period of aging due to the retardation of the precipitation of σ phase.

References

1. C. J. Park and H. S. Kwon, *Corros. Sci.*, 44, 2817 (2002).
2. R. F. Steigerwald, *Corrosion*, 33, 338 (1977).
3. J. O. Nilsson, *Mater. Sci. Tech.*, 8, 685 (1992).
4. C. S. Barret and T. B. Massalski, Structures and Metals, 3rd ed., Oxford, U. K. Pergamon Press, p. 266, (1980).
5. R. G. Barrows and J. B. Newkirk, *Metall. Trans.* 3, 2889 (1972).
6. J. O. Nilsson and A. Wilson, *Mater. Sci. Tech.* 9, 545 (1993).
7. M. E. Williams, V. J. Gadgil, J. M. Krougman, and F. P. Ijsseling, *Corros. Sci.* 36, 871 (1994).
8. K. Ravindranath and S. N. Malhotra, *Corros. Sci.* 37, 121 (1995).
9. K. Ravindranath and S. N. Malhotra, *Corrosion*, 50, 318 (1994).
10. J. S. Kim and H. S. Kwon, *Corrosion*, 55, 512 (1999).
11. G. T. Burnstein, P. C. Pistorius, and S. P. Mattin, *Corros. Sci.* 35, 57 (1993).
12. D. L. Reichert, Electrochemical noise measurement for corrosion applications, ASTM STP 1277, Jeffery R. Kearns, John R. Scully, Pierre R. Roberge, David L. Reichert, and John L. Dawson, Eds., p. 79 (1996).
13. P. C. Pistorius, Electrochemical noise measurement for corrosion applications, ASTM STP 1277, Jeffery R. Kearns, John R. Scully, Pierre R. Roberge, David L. Reichert, and John L. Dawson, Eds., p.343 (1996).
14. H. Böhni, T. Suter, and A. Schreyer, *Electrochim. Acta* 40, 1361 (1995).
15. S. Haykin, Adaptive Filter Theory, second ed., Prentice Hall, Engelwood Cliffs, NJ, p. 798 (1991).
16. V. M. Salinas-Bravo and R. C. Newman, *Corros. Sci.* 36, 67 (1994).
17. J. Hubrecht, R. -W Bosch, J. Chen, W. Bogaerts, and J. H. Zheng, Proceedings, Vol. 1, The 11th Asian-Pacific Corrosion Conference, Ho chi minh, Vietnam, p. 126 (1999).
18. V. T. Borisov, V. M. Golikov, and G. V. Sherbedinskiy, *Phys. Met. Metallogr.* 22, 175 (1996).
19. H. M. Lee, S. M. Allen, and M. Grujicic, *Met. Trans.* 22A, 2869, (1991).
20. J. E. Shackelford, W. Alexander, and J. S.Park, Materials Science and Engineering Handbook, second ed., CRC Press, Boca Raton, FL, p. 219 (1994).